Enhancement of near-infrared absorption in graphene with metal gratings

B. Zhao, J. M. Zhao, and Z. M. Zhang

Articles you may be interested in

Antenna-coupled microcavities for enhanced infrared photo-detection
Appl. Phys. Lett. 104, 031113 (2014); 10.1063/1.4862750

Polarization dependence of photocurrent in a metal-graphene-metal device
Appl. Phys. Lett. 101, 073103 (2012); 10.1063/1.4745787

Layer dependent mechanical responses of graphene composites to near-infrared light
Appl. Phys. Lett. 100, 073108 (2012); 10.1063/1.3685479

Enhanced infrared light harvesting of inorganic nanocrystal photovoltaic and photodetector on graphene electrode
Appl. Phys. Lett. 98, 263509 (2011); 10.1063/1.3605682

Metal–Ge-Si heterostructures for near-infrared light detection
J. Vac. Sci. Technol. B 17, 465 (1999); 10.1116/1.590577

Enhancement of near-infrared absorption in graphene with metal gratings

B. Zhao,[1] J. M. Zhao,[1,2] and Z. M. Zhang[1,a)]

[1]*G.W. Woodruff School of Mechanical Engineering, Georgia Institute of Technology, Atlanta, Georgia 30332, USA*
[2]*School of Energy Science and Engineering, Harbin Institute of Technology, Harbin, People's Republic of China*

Graphene has been demonstrated as a good candidate for ultrafast optoelectronic devices. However, graphene is essentially transparent in the visible and near infrared with an absorptivity of 2.3%, which has largely limited its application in photon detection. This Letter demonstrates that the absorptance in a monatomic graphene layer can be greatly enhanced to nearly 70%, thanks to the localized strong electric field resulting from magnetic resonances in deep metal gratings. Furthermore, the resonance frequency is essentially not affected by the additional graphene layer. The method presented here may benefit the design of next-generation graphene-based optical and optoelectronic devices. © 2014 AIP Publishing LLC. [http://dx.doi.org/10.1063/1.4890624]

Graphene is a two-dimensional monatomic layer of carbon material with tremendous applications because of its unique electric and optical properties.[1–3] Its linear energy dispersion relation implies a vanishing of the effective mass of the carriers, and a remarkably high carrier mobility greater than $200\,000\ \mathrm{cm^2\ V^{-1}\ s^{-1}}$ at room temperature for both electrons and holes.[1] This high mobility makes graphene a great candidate for ultrafast optoelectronic devices such as transistors[4] and photodetectors[5–8] in the visible and near-infrared (NIR) range. For applications such as liquid-crystal displays and light-emitting diodes, graphene is used as a transparent conductor and a weak optical absorption is preferred.[9,10] For photon detection, however, a strong absorption is desired in order to generate a large amount of electron-hole pairs and produce a large photocurrent.[7,11–13] High absorption is also preferred for graphene-based optical antennas[14] and solar cells.[15]

In the long wavelength range (i.e., mid- to far-infrared), the optical properties of graphene resemble those of Drude-type materials,[16,17] and thus plasmonic resonance can be employed to create strong resonance absorption.[17–19] On the contrary, in the visible and NIR range, graphene has no plasmonic response but has a wavelength-independent absorptivity of about 2.3%, which can be related to the fine structure constant as demonstrated experimentally by Nair et al.[20] Therefore, absorption enhancement is highly desirable for graphene-based photon detection. One method to enhance graphene absorption is to employ a microcavity that enables light to pass through the graphene sheet multiple times.[7,21] However, very few studies have considered the enhancement of graphene using nanostructures.[8,14,22]

In this Letter, a method of enhancing the absorptance of graphene is presented by using a deep metallic grating, which can enable a strong localized electric field at the magnetic resonances or magnetic polaritons (MPs). The structure is illustrated in Fig. 1(a), where a single sheet of graphene is laid atop a silver (Ag) deep grating. In the visible and NIR region, graphene behaves as a pure conductor or resistor that can absorb a large amount of the electromagnetic energy at the trench opening. Furthermore, the MP resonance frequency or wavelength is essentially not affected by the graphene overlay. Therefore, the wavelength at which the graphene absorption is enhanced can be tailored by tuning the geometry of the grating. The mechanism of graphene absorption augment based on MPs in deep gratings is different from those based on localized plasmonic resonances,[8,14] or guided resonance in photonic crystals.[22]

As shown in Fig. 1(a), the one-dimensional (1D) grating has the following geometric parameters: period Λ, height h, and trench width b. The Ag region below the grating is assumed to be sufficiently thick for it to be opaque. The optical constants of Ag are modeled with a Drude model.[23,24] The overall absorptance can be obtained from $\alpha = 1 - R$, where the reflectance R was calculated by the rigorous coupled-wave analysis (RCWA).[24] Figure 1(b) shows the absorptance for transverse magnetic (TM) waves at normal incidence ($\theta = 0°$) with $\Lambda = 400\,\mathrm{nm}$, $h = 200\,\mathrm{nm}$, and $b = 30\,\mathrm{nm}$ with and without a graphene overlay. Two absorption peaks can be seen at $6705\,\mathrm{cm^{-1}}$ (wavelength $\lambda = 1.49\,\mu\mathrm{m}$) and $18\,490\,\mathrm{cm^{-1}}$ ($\lambda = 541\,\mathrm{nm}$), which are the first and second MP modes, respectively, identified as MP1 and MP2 in the figure. With the addition of the graphene sheet, the overall absorptance is raised from 0.21 to 0.81 at MP1 and from 0.62 to 0.99 at MP2, without changing the MP resonance frequencies. The difference cannot be attributed to the absorption by graphene since free-standing graphene cannot absorb more than 2.3% of the incident electromagnetic energy. The coupling mechanism and the absorption distribution are explored in the following.

In the simulation, the graphene layer is modeled as a thin sheet of thickness $\Delta = 0.3\,\mathrm{nm}$ with an equivalent dielectric function $\varepsilon(\omega) = i\sigma_s(\omega)/(\varepsilon_0 \omega \Delta)$,[3] where ε_0 is the vacuum permittivity and ω is the angular frequency. Here, $\sigma_s = \sigma_D + \sigma_I$ is the sheet conductance that is modeled as a sum of a Drude (intraband) term and an interband term, viz.,

a)Author to whom correspondence should be addressed. Electronic mail: zhuomin.zhang@me.gatech.edu. Tel.: (404) 385-4225. Fax: (404) 894-8496.
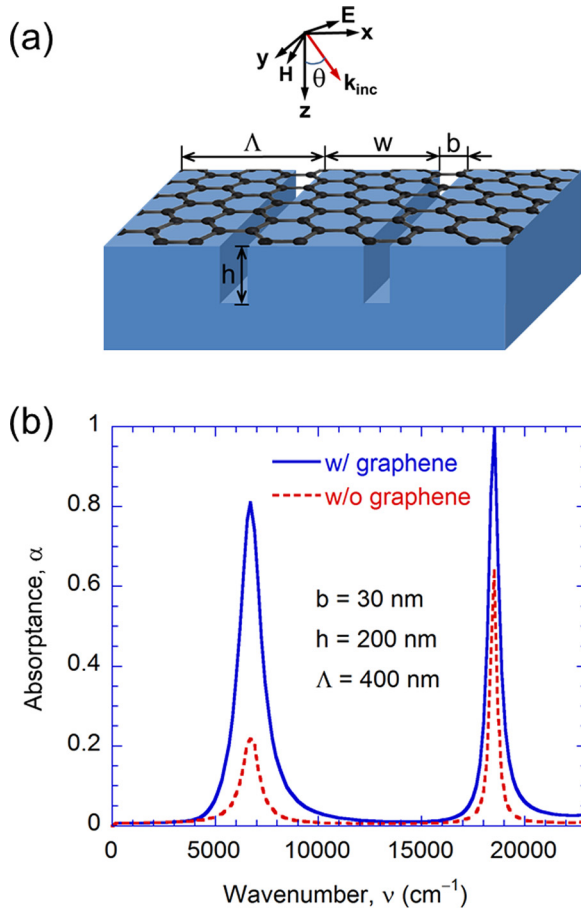
FIG. 1. (a) Schematic of the graphene-covered deep Ag grating. (b) Comparison of the normal absorptance of the graphene-covered (with graphene) and plain (w/o graphene) Ag deep grating with $h = 200$ nm, $\Lambda = 400$ nm, $b = 30$ nm.

$$\sigma_D = \frac{i}{\omega + i/\tau} \frac{2e^2 k_B T}{\pi \hbar^2} \ln\left[2\cosh\left(\frac{\mu}{2k_B T}\right)\right], \qquad (1)$$

and

$$\sigma_I = \frac{e^2}{4\hbar}\left[G\left(\frac{\hbar\omega}{2}\right) + i\frac{4\hbar\omega}{\pi}\int_0^\infty \frac{G(\xi) - G(\hbar\omega/2)}{(\hbar\omega)^2 - 4\xi^2}d\xi\right], \qquad (2)$$

where $G(\xi) = \sinh(\xi/k_B T)/[\cosh(\mu/k_B T) + \cosh(\xi/k_B T)]$.[16] In Eqs. (1) and (2), e is the electron charge, $\hbar$ is the reduced Planck constant, and k_B is the Boltzmann constant. The parameters used in the calculations are: chemical potential $\mu = 0.3$ eV, relaxation time $\tau = 10^{-13}$ s, and temperature $T = 300$ K.

Figure 2 displays the absorptance contours for TM waves as a function of wavenumber and trench width b, where $\Lambda = 400$ nm and $h = 200$ nm are fixed. The bright bands indicate the MP resonances of different orders. For plain gratings, since a strong field coupling between the two walls of the trench can only happen when the trench is very small,[23] the absorptance decreases drastically as b is widened especially for MP1, at which the absorptance becomes less than 0.1 when $b > 60$ nm. However, for the graphene-covered grating, the absorption remains strong for both MP1 and MP2 resonances even with a large b. Meanwhile, the resonance frequencies are not affected by the additional
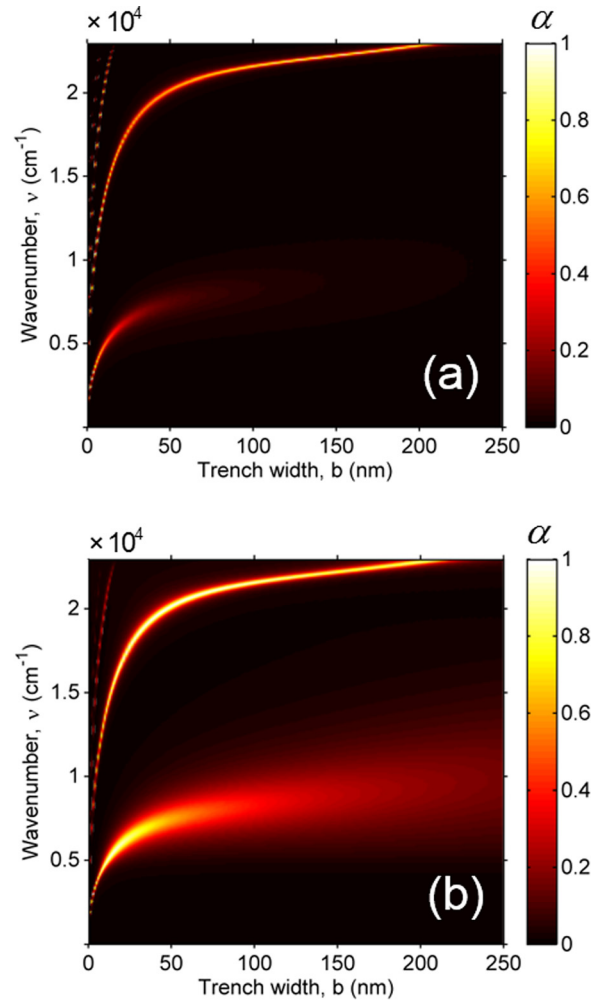

FIG. 2. Absorptance contour for the two structures with $h = 200$ nm and $\Lambda = 400$ nm for varying b: (a) plain Ag grating; (b) graphene-covered Ag grating.

graphene layer but can be tuned by geometric modifications. Furthermore, the bandwidth of the resonance peak becomes broader with the graphene overlay, especially for MP1 at large trench widths. Higher orders of MP can also be
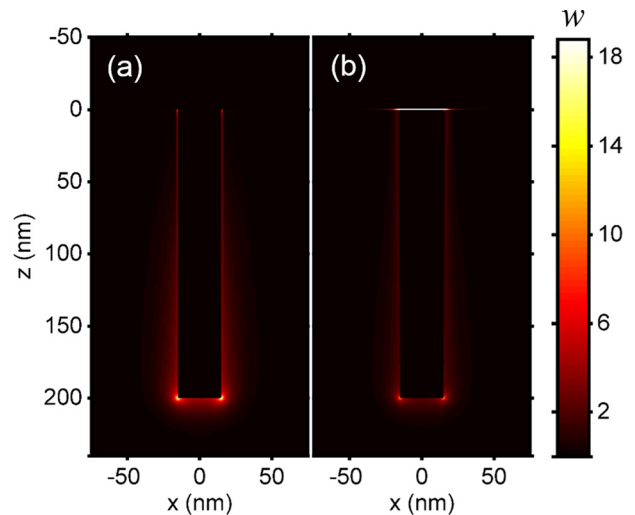

FIG. 3. Power dissipation profile for the two structures at $\lambda = 1.49$ μm: (a) plain Ag grating; (b) graphene-covered Ag grating. The unit of w is 10^4 W/m^3, and the scale bar is not linear beyond 1.8×10^5 W/m^3.

identified in the contour plots, but the focus here is on the fundamental MP or MP1 enhancement since the mechanisms will be similar. Note that transverse electric (TE) waves are not considered since they cannot excite magnetic polaritons for 1D grating.

In order to separate the absorption by the graphene and that by the grating, it is critical to determine where the energy is absorbed or dissipated. The power dissipation density (W/m^3) in a nanostructure can be defined as[25,26]

$$w(x,z) = \frac{1}{2}\varepsilon_0\omega\varepsilon''(x,z)|\mathbf{E}(x,z)|^2, \tag{3}$$

where ε'' is the imaginary part of the dielectric function and $\mathbf{E}$ is the electric field. Note that the magnetic loss is not involved because all the materials considered are nonmagnetic. The power dissipation profile at MP1 resonance ($\lambda = 1.49\,\mu m$) for the two structures with the same geometries as Fig. 1(b) are depicted in Fig. 3. Note that $z = 0$ is at the surface of the grating and $x = 0$ is the symmetry plane of the structure. In the RCWA calculation, the magnitude of the incident electric field is set to unity. Comparing Fig. 3(b) with 3(a), it is clear that the absorption in the Ag walls delineating the trench is not enhanced, but somewhat weakened by the added graphene layer. However, the local absorption in the graphene sheet across the opening of the trench is extremely strong with a maximum w on the order of 10^8 W/m^3, which is three orders of magnitude higher than the highest w in the grating region.

The absorptance can be calculated by the ratio of the total absorbed power within a volume V to the incoming power through the exposed surface area A as follows:[26]

$$\alpha = \frac{\iiint w(x,z)dV}{\frac{1}{2}c_0\varepsilon_0|\mathbf{E}_{inc}|^2 A\cos\theta}, \tag{4}$$

where c_0 is the speed of light in vacuum and the denominator is the product of the Poynting vector and the projected surface area. For the 1D structures discussed here, the volume integration is carried out in the x and z directions only, since the y dimensional length is canceled out. Due to periodicity, the integration length in the x direction can be set to a period as long as A is set equal to Λ. In carrying out the integration, the range $0\,nm \le z \le 300\,nm$ is chosen, because of the small penetration depth of about 46 nm in Ag at $\lambda = 1.49\,\mu m$.[24]

By evaluating Eq. (4), the absorptance for a plain grating is $\alpha = 0.21$, which is the same as the previous obtained value using $1 - R$. When covered by a graphene layer, the absorptance by the Ag grating itself is only 0.13, while that by the graphene sheet is 0.68, which is nearly 30 times higher than the absorptance of a free-standing graphene sheet. Again, the value of $1 - R = 0.81$ is recovered by the sum of the absorptance values of the Ag grating and graphene. Thus, for the graphene-covered grating, most of the incoming power is absorbed by the graphene layer. This could not be possible without the local electric field enhancement by the magnetic resonance or the unique optical properties of graphene in this wavelength range.

Magnetic resonance is realized by a closed current loop induced by the magnetic field of the incident wave.[23,27,28]

Figure 4 shows the electric and magnetic fields at the resonance wavelength of MP1 for the two structures. The color contour represents the square of the magnetic field, and the arrows indicate the direction and relative magnitude of the instantaneous electric field. As the figure shows, a strong magnetic field is confined in the trenches for both structures, though the field enhancement is somehow weaker for the covered grating (see the scale bar). The electric field near the opening of the trench is enhanced to about 20 times greater than that of the incidence in the case shown in Fig. 4(b). This strongly enhanced electric field, as mentioned before, is critical to enabling the graphene to absorb most of the incident power.

Following the induced current loop around the trench, the MP resonance in deep gratings can be described by an inductor-capacitor (LC) circuit model as shown in Ref. 23, where the metal grating severs as an inductor with an inductance L_{Ag} and the trench acts like a capacitor with a capacitance C. One can obtain the fundamental resonance wavelength for the uncovered grating as $\lambda_{MP} = 2\pi c_0\sqrt{CL_{Ag}}$. To consider the effect of graphene on the resonance, additional impedance should be added into the LC circuit. Figure 3(b) suggests that only the graphene across the trench opening may be involved in the effective circuit. The additional impedance introduced by the graphene layer can be evaluated by

$$Z_G = R_G + i\omega L_G = b/\sigma_s. \tag{5}$$

Figure 5 shows the real and imaginary part of the impedance of the graphene sheet, where the inset shows the modified LC circuit for the graphene-covered grating. Note that σ_s is dominated by the interband contribution σ_I, when the photon energy is greater than the interband threshold 2μ.[29] Taking
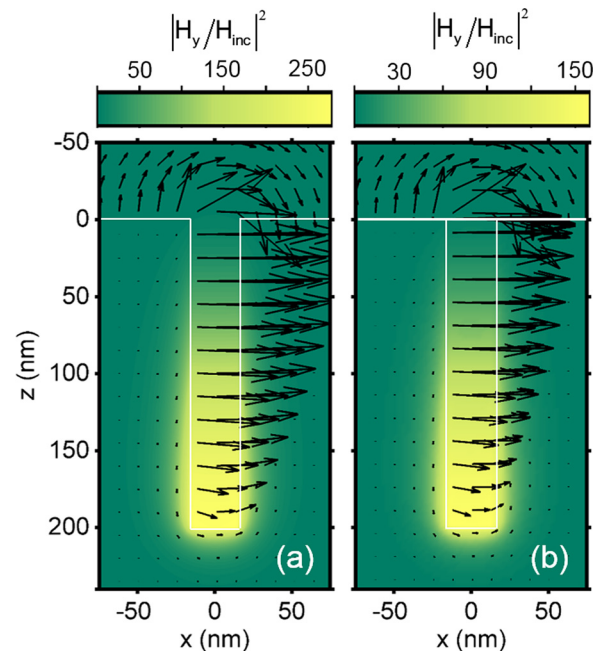

FIG. 4. Electromagnetic field for the two structures at the resonance wavelength $\lambda = 1.49\,\mu m$. The arrows show the direction and relative magnitude of the instantaneous electric field, and the color indicates the square of the magnetic field: (a) plain Ag grating; (b) graphene-covered Ag grating.
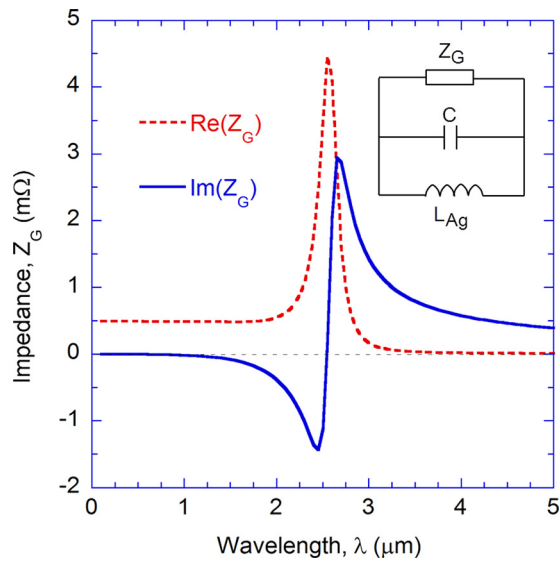
FIG. 5. The impedance of graphene in the LC circuit model versus wavelength.

$\mu = 0.3$ eV, this corresponds to a wavelength of about 2.1 μm. Therefore, at the MP1 resonance wavelength 1.49 μm, $\sigma_s \approx e^2/4\hbar$ is a constant.[20] Subsequently, the impedance becomes a pure resistance $R_G = 4.9 \times 10^{-4}\Omega$. This makes the graphene layer behave like a pure resistor across the trench, where a strongly enhanced local electric field exists when MPs are excited. The time-averaged dissipated power by the resistor element may also be estimated by

$$\langle P_{abs} \rangle = \frac{1}{2R_G} \left| \int_{-b/2}^{b/2} E_x(x) dx \right|^2. \quad (6)$$

Here, only the x-component of the electric field is used since the z-component is negligibly small in the graphene layer. Because the graphene layer is very thin, the electric field is almost independent of z inside graphene. The estimated absorptance can be obtained by dividing Eq. (6) by the incidence power, yielding a value of 0.67 that agrees well with the exact value of 0.68 based on Eq. (4). Therefore, the graphene across the trench opening absorbs nearly 70% of the incoming radiative energy.

Furthermore, since R_G is large, the imaginary part of the total impedance of the circuit shown in Fig. 5 does not change with the graphene overlay. Therefore, the resonance wavelength can still be expressed as $\lambda_{MP} = 2\pi c_0 \sqrt{CL_{Ag}}$ even with the presence of graphene. However, the graphene layer does add resistance to the circuit, making the resonance peaks broader (lower Q factor). Since the resonance wavelengths of MPs in the grating can be controlled by tuning the geometries of the grating such as the height and width,[23] the method presented here can be used to enhance graphene absorption at the wavelength of interest in the NIR or even visible region.

In summary, the enhanced absorption in graphene enabled by deep metal gratings is demonstrated. Since the unique properties of graphene in the NIR range, it serves as

an electric resistor across the opening of the trench, where there is a strong localized electric field when MP modes are excited. The combined effect gives rise to a strongly localized absorption in graphene without affecting the original resonance frequency of the grating. This finding may facilitate the design of graphene-based optical and optoelectronic devices.

[1]K. S. Novoselov, A. K. Geim, S. V. Morozov, D. Jiang, Y. Zhang, S. V. Dubonos, I. V. Grigorieva, and A. A. Firsov, Science **306**, 666 (2004).
[2]F. Xia, H. Yan, and P. Avouris, Proc. IEEE **101**, 1717 (2013).
[3]A. Vakil and N. Engheta, Science **332**, 1291 (2011).
[4]M. Engel, M. Steiner, A. Lombardo, A. C. Ferrari, H. v. Löhneysen, P. Avouris, and R. Krupke, Nat. Commun. **3**, 906 (2012).
[5]F. Xia, T. Mueller, Y.-m. Lin, A. Valdes-Garcia, and P. Avouris, Nat. Nanotechnol. **4**, 839 (2009).
[6]T. Mueller, F. Xia, and P. Avouris, Nat. Photonics **4**, 297 (2010).
[7]M. Furchi, A. Urich, A. Pospischil, G. Lilley, K. Unterrainer, H. Detz, P. Klang, A. M. Andrews, W. Schrenk, G. Strasser, and T. Mueller, Nano Lett. **12**, 2773 (2012).
[8]Z. Fang, Z. Liu, Y. Wang, P. M. Ajayan, P. Nordlander, and N. J. Halas, Nano Lett. **12**, 3808 (2012).
[9]S. Bae, H. Kim, Y. Lee, X. Xu, J.-S. Park, Y. Zheng, J. Balakrishnan, T. Lei, H. Ri Kim, Y. I. Song, Y.-J. Kim, K. S. Kim, B. Ozyilmaz, J.-H. Ahn, B. H. Hong, and S. Iijima, Nat. Nanotechnol. **5**, 574 (2010).
[10]J. Wu, M. Agrawal, H. A. Becerril, Z. Bao, Z. Liu, Y. Chen, and P. Peumans, ACS Nano **4**, 43 (2010).
[11]C.-H. Liu, Y.-C. Chang, T. B. Norris, and Z. Zhong, Nat. Nanotechnol. **9**, 273 (2014).
[12]T. J. Echtermeyer, L. Britnell, P. K. Jasnos, A. Lombardo, R. V. Gorbachev, A. N. Grigorenko, A. K. Geim, A. C. Ferrari, and K. S. Novoselov, Nat. Commun. **2**, 458 (2011).
[13]B. Y. Zhang, T. Liu, B. Meng, X. Li, G. Liang, X. Hu, and Q. J. Wang, Nat. Commun. **4**, 1811 (2013).
[14]Y. Yao, M. A. Kats, R. Shankar, Y. Song, J. Kong, M. Loncar, and F. Capasso, Nano Lett. **14**, 214 (2014).
[15]X. Miao, S. Tongay, M. K. Petterson, K. Berke, A. G. Rinzler, B. R. Appleton, and A. F. Hebard, Nano Lett. **12**, 2745 (2012).
[16]L. A. Falkovsky, J. Phys.: Conf. Ser. **129**, 012004 (2008).
[17]R. Alaee, M. Farhat, C. Rockstuhl, and F. Lederer, Opt. Express **20**, 28017 (2012).
[18]A. Y. Nikitin, F. Guinea, F. J. Garcia-Vidal, and L. Martin-Moreno, Phys. Rev. B **85**, 081405 (2012).
[19]S. Thongrattanasiri, F. H. L. Koppens, and F. J. García de Abajo, Phys. Rev. Lett. **108**, 047401 (2012).
[20]R. R. Nair, P. Blake, A. N. Grigorenko, K. S. Novoselov, T. J. Booth, T. Stauber, N. M. R. Peres, and A. K. Geim, Science **320**, 1308 (2008).
[21]A. Ferreira, N. M. R. Peres, R. M. Ribeiro, and T. Stauber, Phys. Rev. B **85**, 115438 (2012).
[22]J. R. Piper and S. Fan, ACS Photonics **1**, 347 (2014).
[23]B. Zhao and Z. M. Zhang, J. Quant. Spectrosc. Radiat. Transfer **135**, 81 (2014).
[24]Z. M. Zhang, *Nano/Microscale Heat Transfer* (McGraw-Hill, New York, 2007).
[25]K.-H. Brenner, Opt. Express **18**, 10369 (2010).
[26]G. Baffou, R. Quidant, and C. Girard, Appl. Phys. Lett. **94**, 153109 (2009).
[27]B. Zhao, L. Wang, Y. Shuai, and Z. M. Zhang, Int. J. Heat Mass Transfer **67**, 637 (2013).
[28]L. P. Wang and Z. M. Zhang, Appl. Phys. Lett. **100**, 063902 (2012).
[29]C. H. Gan, H. S. Chu, and E. P. Li, Phys. Rev. B **85**, 125431 (2012).